Miao, Lijuan et al.

**Article — Published Version**

# Future drought in the dry lands of Asia under the 1.5 and 2.0 °C warming scenarios

Earth's Future

Earth's Future

RESEARCH ARTICLE
10.1029/2019EF001337

**Key Points:**
- Future global climate change will impose severe drought issues in dryland Asia, including drying trends and expanded arid areas
- Drought conditions in dryland Asia under the 2.0 °C warming will not be as severe as those under the 1.5 °C warming
- Future drought conditions in Kazakhstan and Northwest China will likely be more severe in dryland Asian countries

**Supporting Information:**
- Supporting Information S1

**Correspondence to:**
F. Zhang,
fengzhang@fudan.edu.cn

**Citation:**
Miao, L., Li, S., Zhang, F., Chen, T., Shan, Y., & Zhang, Y. (2020). Future drought in the dry lands of Asia under the 1.5 and 2.0 °C warming scenarios. *Earth's Future*, *8*, e2019EF001337. https://doi.org/10.1029/2019EF001337

Received 28 AUG 2019
Accepted 16 APR 2020
Accepted article online 19 APR 2020
Corrected 16 JUN 2020

This article was corrected on 16 JUN 2020.



# Future Drought in the Dry Lands of Asia Under the 1.5 and 2.0 °C Warming Scenarios

**Lijuan Miao[1,2], Suyuan Li[3], Feng Zhang[4], Tiexi Chen[1], Yunpeng Shan[5], and Yushan Zhang[3]**

[1]School of Geographical Sciences, Nanjing University of Information Science and Technology, Nanjing, China, [2]Leibniz Institute of Agricultural Development in Transition Economies (IAMO), Halle (Saale), Germany, [3]Key Laboratory of Meteorological Disaster, School of Atmospheric Sciences, Nanjing University of Information Science and Technology, Nanjing, China, [4]Department of Atmospheric and Oceanic Sciences & Institute of Atmospheric Sciences, Fudan University, Shanghai, China, [5]Department of Atmospheric Science, University of Wyoming, Laramie, WY, USA

**Abstract** Drought has become a major threat to local sustainable development in dryland Asia, one of the largest grassland ecosystems in the world. However, empirical- and science-based evidence regarding the extent of drought changes and the future trends of these changes in dryland Asia is variable and incomplete. Here, we first investigate the historical variations in drought conditions in dryland Asia, as measured by the drought intensity and arid area, using three widely used drought indices (the Palmer Drought Severity Index, the Standardized Precipitation Index, and the Standardized Precipitation Evapotranspiration Index). Then, we use Bayesian model averaging to reproduce the future drought conditions under two representative concentration pathways (RCP2.6 and RCP4.5) from the Coupled Model Intercomparison Project Phase 5 Earth system models. The Palmer Drought Severity Index, Standardized Precipitation Index, and Standardized Precipitation Evapotranspiration Index illustrate that dryland Asia has experienced an overall drying trend and an expansion of arid areas over the past 100 years (1901–2016). Both temperature and precipitation are projected to increase under both the 1.5 and 2.0 °C warming scenarios compared with the values from the reference period (1986–2005). The projected drought conditions in the 1.5 and 2.0 °C warming scenarios will worsen, especially across Kazakhstan and Northwest China. We found that the drought conditions under the 2.0 °C warming conditions will not be as severe as those under the 1.5 °C warming conditions due to the mitigating effect of the projected precipitation increase under RCP4.5. These results call for short-term and long-term mitigation and adaptation measurements for drought events in dryland Asia.

**Plain Language Summary** To avoid the negative impacts of climate warming, the Paris Agreement aims to pursue efforts to maintain the global warming increase at well below 1.5 and even 2.0 °C until the end of the century. Questions have been raised regarding the climate extremes in dryland Asia. Will drought issues become more severe under the context of global warming? Are the existing drought indices able to quantify and characterize the drought intensity and arid area in this region? Answers to these questions are crucial for the livelihood of millions of individuals, as these people rely on grassland biomass to feed both animals and farmers; however, the answers remain unclear. Here, we found that the projected drought severity and arid area will persistently increase under both the 1.5 and 2.0 °C global warming scenarios. We also found that the drought conditions under the 2.0 °C warming scenario will be mitigated relative to those under the 1.5 °C warming scenario due to the beneficial effect of adequate precipitation under representative concentration pathway 4.5. Kazakhstan and Northwest China might be severely affected by drought. Therefore, understanding future changes in drought conditions in dryland Asia is critical for developing adaptation measures to cope with the challenges of rapid climate change.

## 1. Introduction

Dry lands provide a suite of ecosystem services, such as recovering vegetation greenness, sequestering soil carbon, providing feed and fodder for livestock, and sustaining biodiversity (Fraser et al., 2011; He et al., 2019). Dryland areas are among the most vulnerable regions to ongoing climate change and climate extremes (Fraser et al., 2011; Huang et al., 2016). Asia has the largest continuous grassland biome in the world, accounting for 38% of the entire Asian land mass (Bai et al., 2007; Miao et al., 2015), which

stretches over $10 \times 10^6$ km$^2$ from the Caspian Sea in the west to Manchuria in the east and covers seven countries, including the five Central Asia countries (Kazakhstan, Uzbekistan, Turkmenistan, Tajikistan, and Kyrgyzstan), Republic of Mongolia, and northwestern China. In dryland Asia, climate change, especially drought, is a growing concern for the sustainable development of local agriculture and animal husbandry (Chen et al., 2013; Sternberg, 2018). In recent decades, both observations and model simulations have suggested that dryland Asia has been exposed to serious pressure from climate change and climate extremes (Trenberth et al., 2013).

During past decades, dryland Asia has experienced climatic warming at a rate far greater than the global average (Miao, et al., 2015). For example, the annual average temperature in Central Asia and the Republic of Mongolia has increased by a decadal average of 0.4 °C during the last 40 years (Hu et al., 2014; Tao et al., 2015). Additionally, limited and volatile precipitation and high evapotranspiration have contributed to increasing aridity and resulted in widespread land degradation, soil erosion, and severe water scarcity (Tao et al., 2015; Wang et al., 2013). Such situations pose direct threats to the livelihoods of millions of herders who rely on the grassland biomass for feeding their animals (Miao et al., 2015; Sneath, 1999). Climate models under different representative concentration pathways (RCPs) are key tools used to obtain knowledge on the trends of future climatic change and the corresponding impact on terrestrial ecosystems (Huang et al., 2018). Future challenges are enormous because the temperature is expected to continuously increase between 2010 and 2100 by an average of 2.9 °C during the vegetation growing season, according to a midrange emission scenario, and precipitation will gradually increase, albeit with large spatial variation and high uncertainty (Miao et al., 2015). Moreover, future climate conditions will likely induce more frequent, severe, and prolonged droughts than currently observed, which will exacerbate land degradation and augment the risks posed to rural livelihoods (Wang et al., 2013).

Many studies have used a single drought index to capture drought characteristics globally and regionally (Brito et al., 2018; Trenberth et al., 2013). However, compared with the results from combined indices, a single drought index might not be able to provide comprehensive and consistent information on drought because climatic conditions vary among regions (Adnan et al., 2017; Chen et al., 2019). In addition, the Paris Agreement aims to limit global mean surface warming to less than 2.0 °C relative to preindustrial levels (Meinshausen et al., 2009). Many studies have assessed the impact of the 1.5 and 2.0 °C warming targets using transient warming scenarios according to the Coupled Model Intercomparison Project Phase 5 (CMIP5) RCPs. For example, the drought risk in the Mediterranean region and central Europe will increase significantly for both the 1.5 and 2.0 °C warming targets (Lehner et al., 2017). Limiting warming to 1.5 °C, relative to 2.0 °C, would reduce the frequency of extreme heat events in Australia and Africa (King et al., 2017; Nangombe et al., 2018). However, empirical, science-based evidence concerning the extent of the changes in drought and the future variations in dryland Asia is variable and incomplete.

In light of this issue, our study aims to achieve the following objectives: (1) evaluate the performance and feasibility of three widely used drought indices (PDSI: the Palmer Drought Severity Index, SPI: the Standardized Precipitation Index, and SPEI: the Standardized Precipitation Evapotranspiration Index) in reproducing historical drought conditions (referred to as the drought intensity and arid area) in dryland Asia over the last 100 years, (2) project the spatiotemporal changes in the drought intensity and arid area over dryland Asia under the 1.5 and 2.0 °C global warming scenarios, and (3) determine if the drought conditions will worsen under the 2.0 °C global warming among dryland Asian countries. Our results could, therefore, substantially advance the knowledge of the current and future changes in drought conditions over dryland Asia, and this information could be used by local residents (herders and farmers), policy makers, and investors to enhance efforts to formulate climate adaptation strategies to drought.

## 2. Materials and Methods

### 2.1. Study Area

Dryland Asia (46–127°E and 31–56°N) comprises typical arid and semiarid lands and stretches over $10 \times 10^6$ km$^2$; dry lands are characterized by frequent drought, low precipitation, and increasing temperature (Miao et al., 2015). Here, dryland Asia is a geographical combination of the five Central Asian countries, the Republic of Mongolia, and six provinces in northwestern China (Figure 1). Land use follows a

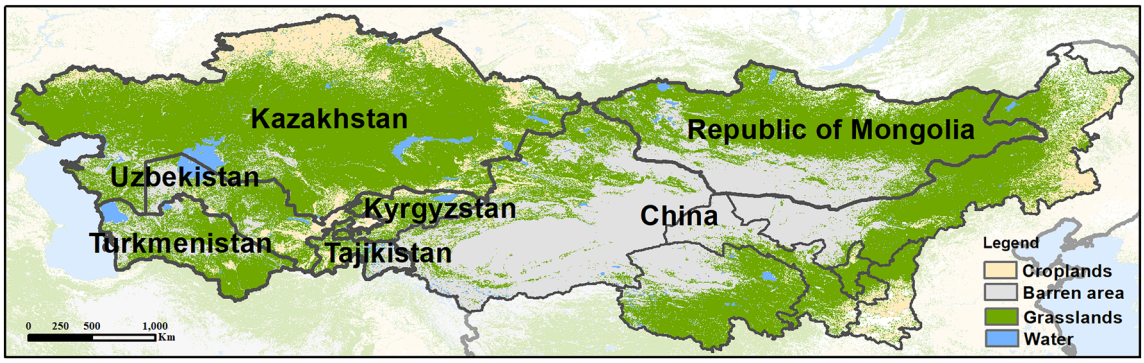


**Figure 1.** Geographical location of dryland Asia.

distribution pattern similar to that of the regional climate. In addition to the croplands in northern dryland Asia, land cover is dominated by grasslands and barren areas (Figure 1).

### 2.2. Data Resources

In this research, we mainly use climate data and global climate projection data, namely, CMIP5 data. The detailed descriptions of the data are as follows.

#### 2.2.1. Climate Data

Climatic Research Unit (CRU) Time Series Version 4.03 is a gridded monthly data set produced by the University of East Anglia (available at: http://data.ceda.ac.uk/badc/cru/data/cru_ts/cru_ts_4.03) (Jones & Harris, 2013). The climatic conditions of the dryland area are effectively represented over a broad with the CRU grid (Wei et al., 2019; Zhang et al., 2017). In this study, we extracted precipitation and temperature data for the period from January 1901 to December 2018 with a spatial resolution of $0.5 \times 0.5°$.

#### 2.2.2. CMIP5 Data

Historical and future simulations of climate change in dryland Asia were inferred from 17 CMIP5 global climate model outputs (available at https://esgf-node.llnl.gov/search/cmip5/) (Table 1), covering the time period from 2006 to 2100. Here, model simulations from two RCPs are considered, namely, RCP2.6 and RCP4.5, which are labeled based on the possible range of radiative forcing values (2.6 and 4.5 $W/m^2$, respectively) in the year 2100 (instead of RCP6.0 and 8.5 because they are too intense); these are the most widely used global warming scenarios that may occur in the future, with potential 1.5 °C (RCP2.6) and 2.0 °C (RCP4.5) changes.

**Table 1**
*Lists of the CMIP5 Climate Models Used in This Study*

| ID | Model name | Resources |
|---|---|---|
| 1 | BCC-CSM1 | Beijing Climate Center, China |
| 2 | BNU-ESM | Beijing Normal University, China |
| 3 | CanESM2 | Canadian Centre for Climate, Canada |
| 4 | CCSM4 | National Center for Atmospheric Research, USA |
| 5 | CSIRO-Mk3-6-0 | Commonwealth Scientific and Industrial Research, Australia |
| 6 | FGOALS-g2 | Institute of Atmospheric and Industrial Research, Australia |
| 7 | FIO-ESM | The First Institute of Oceanography, SOA, China |
| 8 | GISS-E2-H | NASA Goddard Institute for Space Studies, USA |
| 9 | GISS-E2-R | NASA Goddard Institute for Space Studies, USA |
| 10 | HadGEM2-AO | Met Office Hadley Centre, UK |
| 11 | IPSL-CM5A-LR | Institute Pierre-Simon Laplace, France |
| 12 | MIROC5 | Atmosphere and Ocean Research Institute, Japan |
| 13 | MIROC-ESM | Japan Agency for Marine-Earth Science and Technology, Japan |
| 14 | MIROC-ESM-CHEM | Japan Agency for Marine-Earth Science and Technology, Japan |
| 15 | MPI-ESM-LR | Max Planck Institute for Meteorology, Germany |
| 16 | MRI-CGCM3 | Meteorological Research Institute, Japan |
| 17 | NorESM1-M | Norwegian Climate Centre, Norway |

### 2.3. Research Methods

#### 2.3.1. Drought Assessment

There are many drought indices that have been developed by meteorologists and climatologists to indicate drought conditions around the world. Here, we applied three commonly used drought indices (the PDSI, SPI, and SPEI) (Dai et al., 2004; Liu et al., 2016; Tian et al., 2018)) to evaluate the historical and future drought conditions over dryland Asia. Drought indices have distinct trends associated with characterizing drought conditions (Chen et al., 2017); here, we chose both physical and statistical drought indices, including the PDSI and SPEI (also SPI). During the calculation process, PET is involved in both the PDSI and SPEI. The PDSI and SPEI are designed to estimate the water balance of the land surface layer, and PET plays an essential role in this balance. The theoretical formula of PET is often difficult to construct in practical applications; therefore, a reference PET is used as a substitute. The SPI can directly reflect the changes in precipitation. Furthermore, when selecting thresholds, different indices might slightly differ in their representation of droughts.

The formulas for each of these indices are listed as follows.

1. The PDSI

The PDSI was created by Palmer in 1965, and it involves four surface water fluxes, namely, evapotranspiration (*ET* or *PET*), recharge to soils (*R* or *PR*), runoff (*RO* or *PRO*), and water loss to the soil layers (*L* or P*L*). Based on the concept of climatically appropriate values for existing conditions, Palmer proposed water balance coefficients ($\alpha_i$, $\beta_i$, $\gamma_i$, and $\delta_i$) for each month $i$ (Wayne, 1965) as

$$\alpha_i = \frac{\overline{ET_i}}{\overline{PET_i}},\ \beta_i = \frac{\overline{R_i}}{\overline{PR_i}},\ \gamma_i = \frac{\overline{RO_i}}{\overline{PRO_i}},\ \text{and}\ \delta_i = \frac{\overline{L_i}}{\overline{PL_i}}. \tag{1}$$

According to the water balance coefficients, the actual precipitation is $P_i$, the climatically appropriate precipitation is $\overline{P_i}$, and the moisture anomaly index is $Z_i$ for each month $I$ and is calculated as follows:

$$PDSI_i = p \times PDSI_{i-1} + q \times Z_i \tag{2}$$

$$Z_i = \left(P_i - \overline{P_i}\right) \times K_i \tag{3}$$

$$\overline{P_i} = \alpha_i PET_i + \beta_i PR_i + \gamma_i PRO_i - \delta_i PL_i \tag{4}$$

where $K_i$ represents the climatic characteristic moisture anomaly index for each month $i$ ($i$ = 1, 2, 3, ..., 12).

2. The SPI

The SPI is flexible and designed to quantify the precipitation deficit at multiple timescales, for example, 1, 3, 6, 12, 24, and 48 months. In this study, we adopted a monthly timescale for each grid because a short-timescale SPI, such as a 1 month SPI, can provide early warnings regarding drought and help assess the drought severity (Svoboda et al., 2012).

$$H(x) = q_0 + (1 - q_0)Gamcaf(P0) \tag{5}$$

$$SPI = \begin{cases} +\left(w - \dfrac{a_0 + a_1 w + a_2 w^2}{1 + b_1 w + b_2 w^2 + b_3 w^3}\right),\ 0.5 < H(x) \le 1\ \text{ and }\ w = \sqrt{\ln\left[1/(H(x))^2\right]} \\ -\left(w - \dfrac{a_0 + a_1 w + a_2 w^2}{1 + b_1 w + b_2 w^2 + b_3 w^3}\right),\ 0 < H(x) \le 0.5\ \text{ and }\ w = \sqrt{\ln\left[1/(1-H(x))^2\right]} \end{cases} \tag{6}$$

where $H(x)$ is the cumulative probability of precipitation, $q_0$ is the probability of zero precipitation, and $P0$ is the precipitation without zero values. The coefficients in equation (6) were set as follows: $a_0$ = 2.516, $a_1$ = 0.8029, $a_2$ = 0.0103, $b_1$ = 1.4328, $b_2$ = 0.1893, and $b_3$ = 0.0013.

3. The SPEI

The SPEI was created by Vicente-Serrano et al. based on both precipitation and temperature. Temperature is not an input parameter in calculating the SPI; however, the SPEI is designed to include a temperature component to address PET. The SPEI is also designed to quantify the precipitation deficit at multiple timescales,

for example, 1, 3, 6, 12, 24, and 48 months. Here, we adopted a monthly timescale for the calculation of the SPEI in each grid.

To calculate PET, we applied the method designed by C.W. Thornthwaite (Thornthwaite, 1948); for details, see formulas (7)–(10).

$$i = [\max(T, 0)]^{1.514} \tag{7}$$

$$I = \sum_{i=1}^{12} i \tag{8}$$

where $T$ is the monthly mean temperature (°C) and $I$ is a heat index, which is calculated as the sum of 12 monthly index values $i$ ($i$ = 1, 2, 3, ..., 12).

$$m = 6.75 \times 10^{-7} I^3 - 7.71 \times 10^{-5} I^2 + 1.79 \times 10^{-2} I + 0.492 \tag{9}$$

$$PET = 16\left(\frac{N}{12}\right)\left(\frac{NDM}{30}\right)\left(\frac{10T}{I}\right)^m \tag{10}$$

$$D_i = P_i - PET_i \tag{11}$$

$$F(x) = \exp\left\{-\left[1-k\left(\frac{x-\mu}{\beta}\right)\right]^{\frac{1}{k}}\right\} \tag{12}$$

$$SPEI = \begin{cases} +\left(w - \dfrac{a_0 + a_1 w + a_2 w^2}{1 + b_1 w + b_2 w^2 + b_3 w^3}\right), & F(x) > 0.5 \text{ and } w = \sqrt{-2\ln[1 - F(x)]} \\ -\left(w - \dfrac{a_0 + a_1 w + a_2 w^2}{1 + b_1 w + b_2 w^2 + b_3 w^3}\right), & F(x) \le 0.5 \text{ and } w = \sqrt{-2\ln F(x)} \end{cases} \tag{13}$$

where $NDM$ is the day number of the month; $N$ is the maximum number of sun hours; $m$, $\beta$, and $k$ are the location, scale, and shape parameters of the gamma distribution, respectively; and the values of $a_0$, $a_1$, $a_2$, $b_1$, $b_2$, and $b_3$ are the same as those for the SPI.

We can see from the above formulas that the SPI is calculated based on precipitation only, and the PDSI and SPEI consider both precipitation- and temperature-related variables. According to the discrepancies in values, we can classify drought into near-normal, moderately dry, severely dry, and extremely dry conditions (Tab. 2) (Svoboda et al., 2012; Wayne, 1965). Specifically, drought events are believed to occur when the PDSI is continuously negative and reaches a value of −2.0 or less. For the SPI/SPEI, a drought event occurs when the SPI/SPEI is consistently negative and reaches a value of −1.0 or less. A drought event ends when these drought indices become positive. Thus, arid areas are defined as regions that are moderately dry, severely dry, and extremely dry.

### 2.3.2. Multimodel Simulations of Future Climatic Change

Theoretically, Bayesian model averaging (BMA) is designed to assign the highest weight to the model that displays the best agreement with observations to obtain the best possible result (Hoeting et al., 1999). Compared with single-model and simple model averaging, BMA has the best potential to represent the future climate conditions in dryland Asia (Miao et al., 2015). Here, we used the CRU data set from 1986 to 2005 as the reference period for the assessment of temperature and precipitation simulations from 17 CMIP5 models. BMA-based weights were thus assigned to these models (the same weight was assigned to pixels belong to the same model). Based on these weights, we obtained future variations in temperature and precipitation for two climate change scenarios (RCP2.6/4.5) from 2006 to 2099.

We also noticed the bias between CMIP5 model simulations (BMA-based results) and CRU data sets during the period of 1901–2005 (Figures 2a and 2c). Therefore, we generated future temperature and precipitation maps by adding the changes based on CMIP5 model projections to the current climate conditions (i.e., climate change), as shown in equation (14).

**Table 2**
*Standard for the Classification of Three Drought Indices*

| Classification | PDSI | SPI/SPEI |
|---|---|---|
| Near normal | −1.99 to 0 | −0.99 to 0 |
| Moderately dry | −2.99 to −2.0 | −1.49 to −1.0 |
| Severely dry | −3.99 to −3.0 | −1.99 to −1.5 |
| Extremely dry | ≤−4.0 | ≤−2.0 |

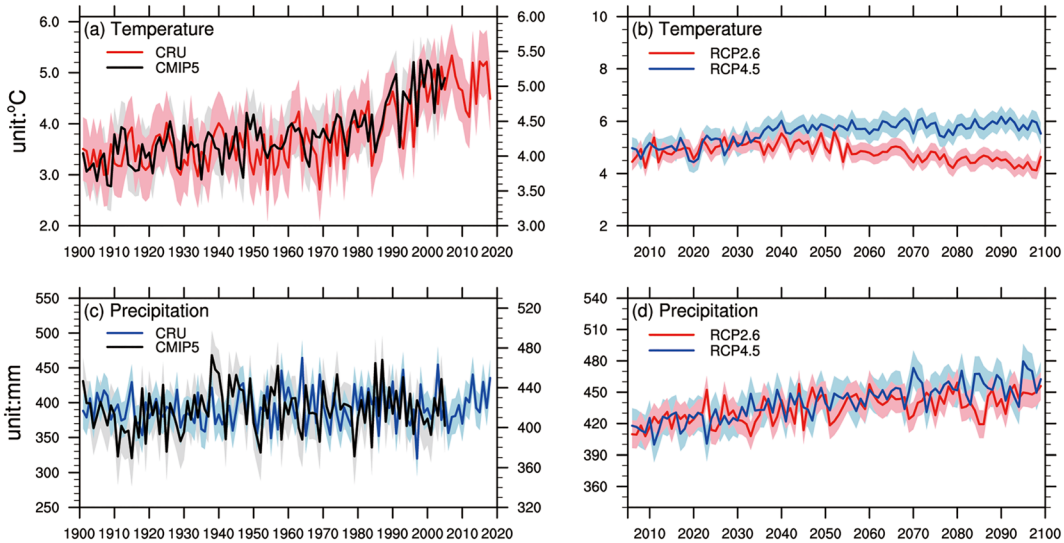


**Figure 2.** Variations in historical and future climatic change in dryland Asia. (a) The annual mean temperature extracted from the CRU data set (1901–2018) and CMIP5 model simulations (1901–2005), (b) the annual mean temperature from 2006 to 2099 from CMIP5 model simulations, (c) the annual total precipitation from the CRU data set (1901–2018) and CMIP5 model simulations (1901–2005), and (d) the annual total precipitation from 2006 to 2099 from CMIP5 model simulations. The solid lines and shaded areas indicate the averages and the corresponding standard deviations, respectively, over the study area.

$$Future_{T,P} = \left(CMIP5_{Future} - CMIP5_{History}\right) + CRU_{History} \tag{14}$$

The global mean annual temperature from 1986–2005 had warmed by 0.61 °C since the preindustrial era according to IPCC, 2013 (IPCC, 2013). If the global mean annual temperature continues to increase by 0.89 or 1.39 °C, the global mean annual temperature will warm by 1.5 or 2.0 °C, respectively. Here, we chose the reference period from 1986 to 2005 based on the CRU data set, which has a high spatial resolution and achieves high performance by considering historical climate. The period of the 1.5 °C global warming scenario is 2020–2039 (2018–2037) under RCP2.6 (RCP4.5) and that for 2.0 °C is 2040–2059 under RCP4.5, as calculated by the 20 year mean annual temperature relative to that in the preindustrial era (Su et al., 2018). Thus, we selected RCP2.6 (low emission scenario) and RCP4.5 (moderate emission scenario) for our predictions; these scenarios are the most widely used global warming scenarios for 1.5 °C (RCP2.6, RCP4.5) and 2.0 °C (RCP4.5) that may occur in the future. We did not select RCP6.0 because it is a moderate emission scenario, much like RCP4.5. Additionally, we did not consider RCP8.5 because it is the 3 °C global warming scenario, and the global mean annual temperature will likely not reach 3–4 °C by the end of 2100 (Noah & Filippo, 2012).

## 3. Results

### 3.1. Historical and Future Climate Change in Dryland Asia

Figures 2a and 2c show the historical annual mean temperature and total precipitation based on CRU and CMIP5 from 1901 to 2018. Based on the CRU data set, the annual mean temperature in dryland Asia increased by 1.7 °C from 1901 to 2018, with a rate of 0.14 °C per decade (Figure 2a). Moreover, the annual total precipitation increased slightly from 388 to 435 mm in the same period (4.0 mm per decade) (Figure 2c). From the CMIP5 model simulations, the annual mean temperature and total precipitation exhibited similar trends over the past century (Figures 2a and 2c). In addition, we projected the future variations in temperature and precipitation for the period of 2006–2099 from the 17 CMIP5 models. The future annual mean temperature will increase by 0.19 and 0.56 °C under RCP2.6 and RCP4.5, respectively (Figure 2b). The rate of increase is 0.02 and 0.06 °C per decade for RCP2.6 and 4.5, respectively. The warming rate in RCP4.5 (0.06 °C per decade) is 3 times faster than that in the previous century (0.02 °C per decade). Additionally, the annual total precipitation will increase slowly from 410/418 to 456/462 mm under RCP2.6/

10.1029/2019EF001337

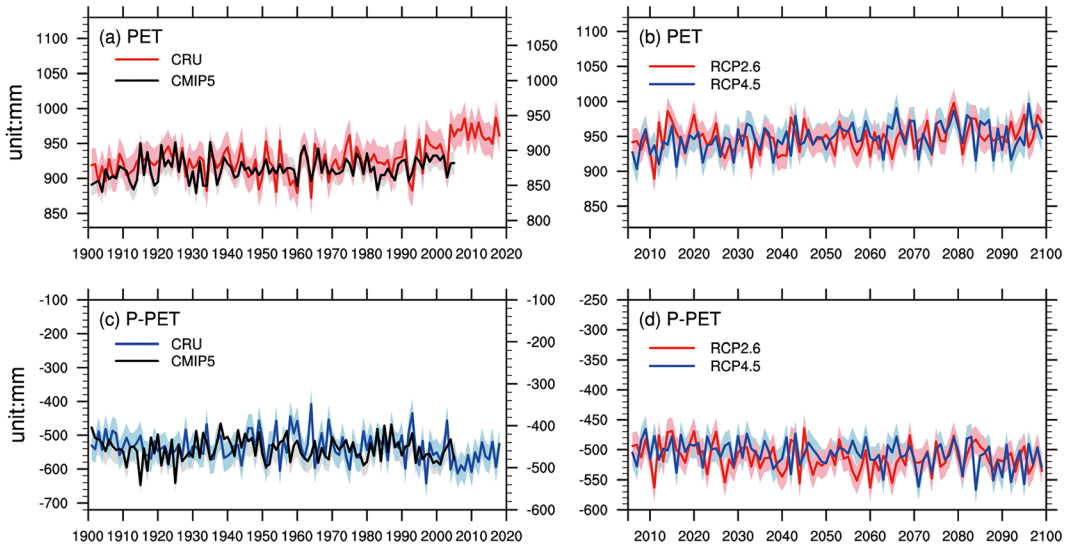


**Figure 3.** Variations in historical and future PET and P-PET in dryland Asia. (a) The annual mean PET from the CRU data set (1901–2018) and CMIP5 model simulations (1901–2005), (b) the annual mean PET from 2006 to 2099 from CMIP5 model simulations, (c) the annual mean P-PET from the CRU data set (1901–2018) and CMIP5 model simulations (1901–2005), and (d) the annual mean P-PET from 2006 to 2099 from CMIP5 model simulations. The solid lines and shaded areas indicate the averages and the corresponding standard deviations, respectively, over the study area.

4.5 from 2006 to 2099 and continue to increase at a rate of 4.9/4.7 mm per decade. RCP4.5 was characterized by higher temperatures and more precipitation compared with RCP2.6, and these changes will likely occur in dryland Asia in the next 100 years.

Moreover, Figure 3 describes PET and P-PET time series in the historical period and in the future in dryland Asia. PET increased from 1901 to 2018, with an obvious increasing trend over dryland Asia, especially for the period of 1990s to 2018, as derived from the CRU and CMIP5 models (Figure 3a). In addition, the P-PET series decreased from 1901 to 2018 (Figure 3c). The previous changes in PET and P-PET inferred from the CRU data set are well captured by the CMIP5 model simulations (Figure 3a and 3c). For the next 100 years, PET will continue to increase slightly, and P-PET will decrease slightly under both RCP2.6 and RCP4.5 (Figure 3b and 3d). We provide the spatial patterns of the linear trends of precipitation, PET, and P-PET from 1986 to 2018 in the c (Figure S1).

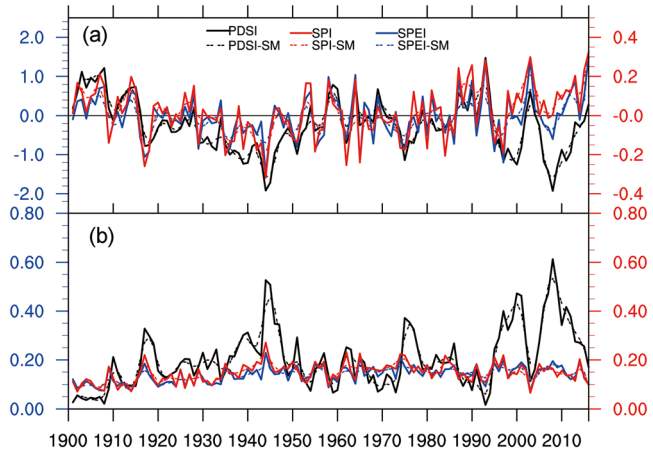


**Figure 4.** Changes in the drought intensity (a) and the percentage of arid area (b), as indicated by the PDSI, SPI, and SPEI in dryland Asia from 1901 to 2016. The left vertical axis shows the results derived from the PDSI, and the right vertical axis shows the results from the SPI and SPEI. The dotted line (PDSI_SM, SPI_SM, and SPEI_SM) is calculated from the cubic smoothing algorithm with a 5-point approximation (Liu et al., 2010).

### 3.2. Spatiotemporal Changes in Historical Drought Conditions

The interannual variations in the drought intensity reflected by the PDSI, SPI, and SPEI are comparable in dryland Asia (Figure 4a). We used the cubic smoothing algorithm developed by Liu et al. with a 5-point approximation and a piecewise linear model (Liu et al., 2010) to detect the linear trend and breakpoint of the drought intensity. The mid-1940s was the average breakpoint for each of the drought indices, which suggested that the drought intensity increased from the 1901 to 1940s and then decreased slightly from the mid-1940s to 2016. In other words, there was a recovery in the drought intensity over dryland Asia after the mid-1940s.

We found good agreement in the proportions of arid areas determined by the three indices, especially those for the SPI and SPEI (Figure 4b). The correlation coefficient between the SPI and SPEI was 0.9, reaching statistical significance at 95%. The proportion of arid areas will increase at rates of 1.5%, 0.4%, and 0.5% per decade for the PDSI, SPI, and SPEI, respectively. Compared with the SPI and SPEI, the PDSI tended to overestimate the proportion of arid area by 6%. The proportion of arid area reached a secondary maximum in 1944, with a value of 53% for the PDSI, and there

10.1029/2019EF001337

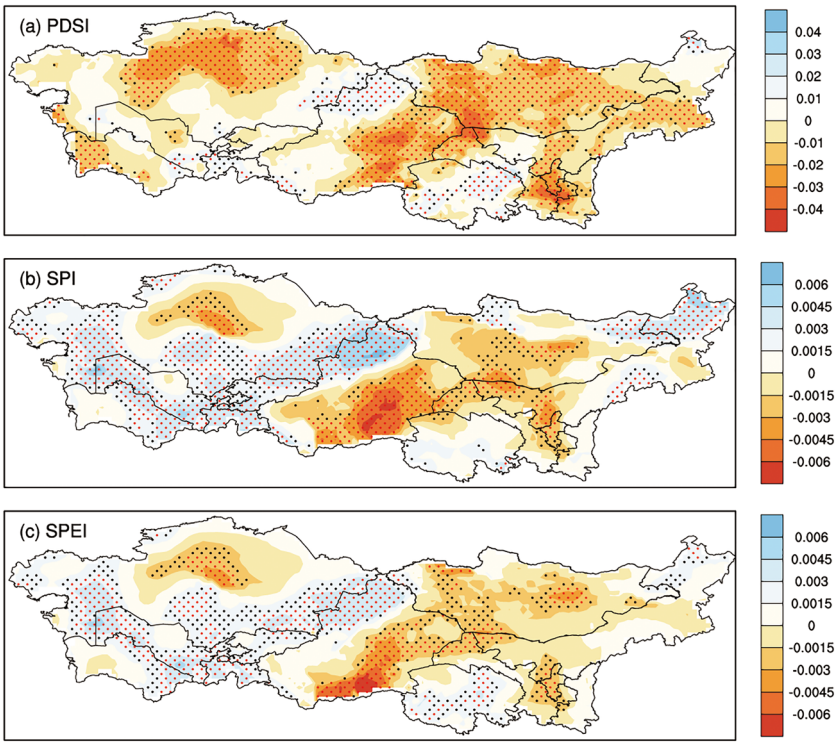


**Figure 5.** Spatial pattern of the linear trend of drought intensity from 1901 to 2016 in dryland Asia, as indicated by the PDSI (a), SPI (b), and SPEI (c). The black and red dotted areas show the regions that experienced significant changes in the drought intensity at the 5% and 1% significance levels, respectively.

was also a peak at 23% for the SPI and at 27% for the SPEI in this year. In addition, for the PDSI, the proportion of arid area reached a zenith at 61% in 2008.

Figure 5 shows the spatial pattern of the linear trends of the drought intensity in dryland Asia from 1901 to 2016. It is obvious that the spatial trends of all indices are roughly similar. Kazakhstan, Mongolia, and Northwest China experienced significantly more severe drought than that experienced in the other countries. Similar with the interannual variations, the increasing trend of drought intensity indicated by the PDSI in dryland Asia from 1901 to 2016 is more severe than the trends indicated by the SPI and SPEI.

### 3.3. Future Changes in Drought Conditions

The future drought conditions characterized by the PDSI, SPI, and SPEI are identical in Figure 6. The drought intensity and the percentage of arid area based on various temperature thresholds were calculated by spatial (in dryland Asia) and temporal averaging (over twenty years). Because the averaging led to fuzzy changes in the PDSI, SPI, and SPEI, the drought intensity trends and the percentages of arid area were characterized by the PDSI, SPI, and SPEI. Compared with the historical period, dryland Asia is projected to experience enhanced drought severity under the 1.5 °C/2.0 °C global warming scenarios, as indicated by all the three drought indices and an enlarged arid area (Figure 6). Unexpectedly, there will be a reduction in the drought intensity and arid area under the 2.0 °C global warming scenario compared with the results of the 1.5 °C global warming scenario (Figure 6).

Figure 7 shows the spatial distributions of the PDSI, SPI, and SPEI in dryland Asia for the reference period and the 1.5 °C/2.0 °C global warming periods. In accordance with Figure 6, Figure 7 shows that there is an obvious increase in the drought intensity and arid area in the two warming scenarios. Compared with the reference period (1986–2005), under the 1.5 °C/2.0 °C global warming scenarios, Kazakhstan and Northwest China generally tended to become dryer.

As jointly indicated by the PDSI, SPI, and SPEI, most of the seven countries are projected to experience increases in the drought intensity and enlarged arid areas (except for Turkmenistan and Mongolia), under

10.1029/2019EF001337

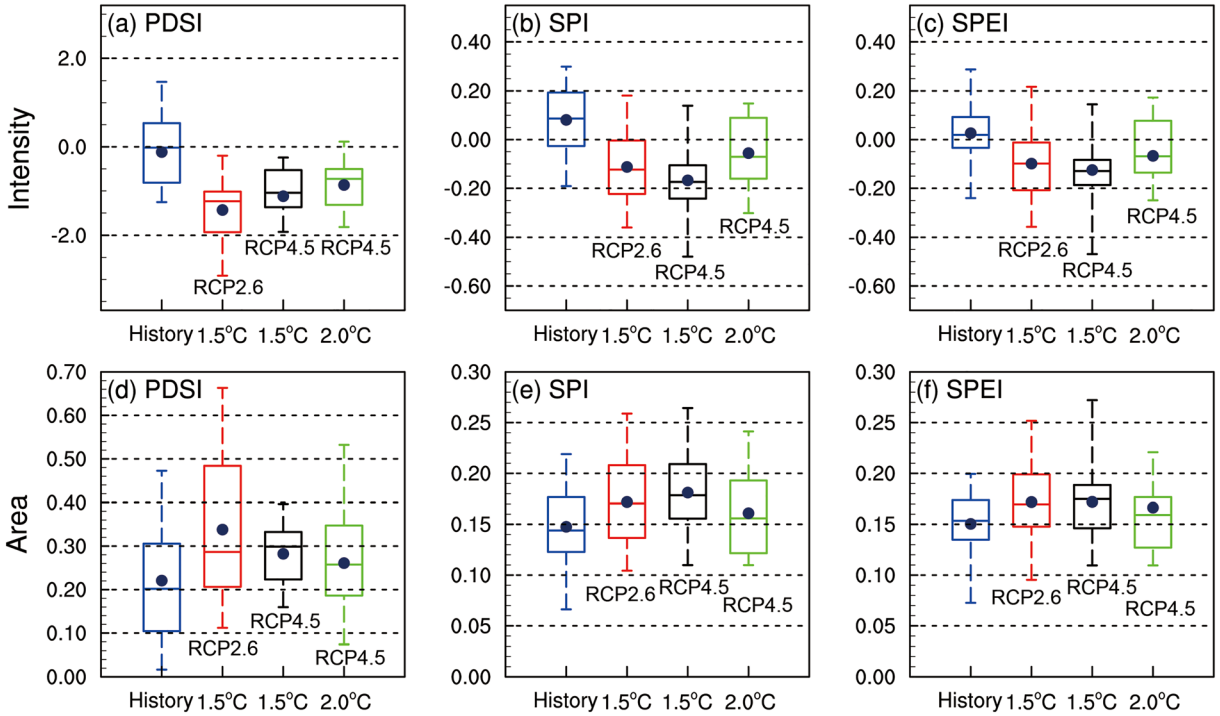


**Figure 6.** Future changes in the drought intensity (a–c) and arid area (d–f) inferred from the PDSI, SPI, and SPEI in dryland Asia for the reference period (1986–2005) and the 1.5 and 2.0 °C global warming periods (RCP2.6: 2020–2039, RCP4.5: 2018–2037, and RCP4.5: 2040–2059) based on CMIP5 model simulations. Negative values of an index indicate dry climate conditions.

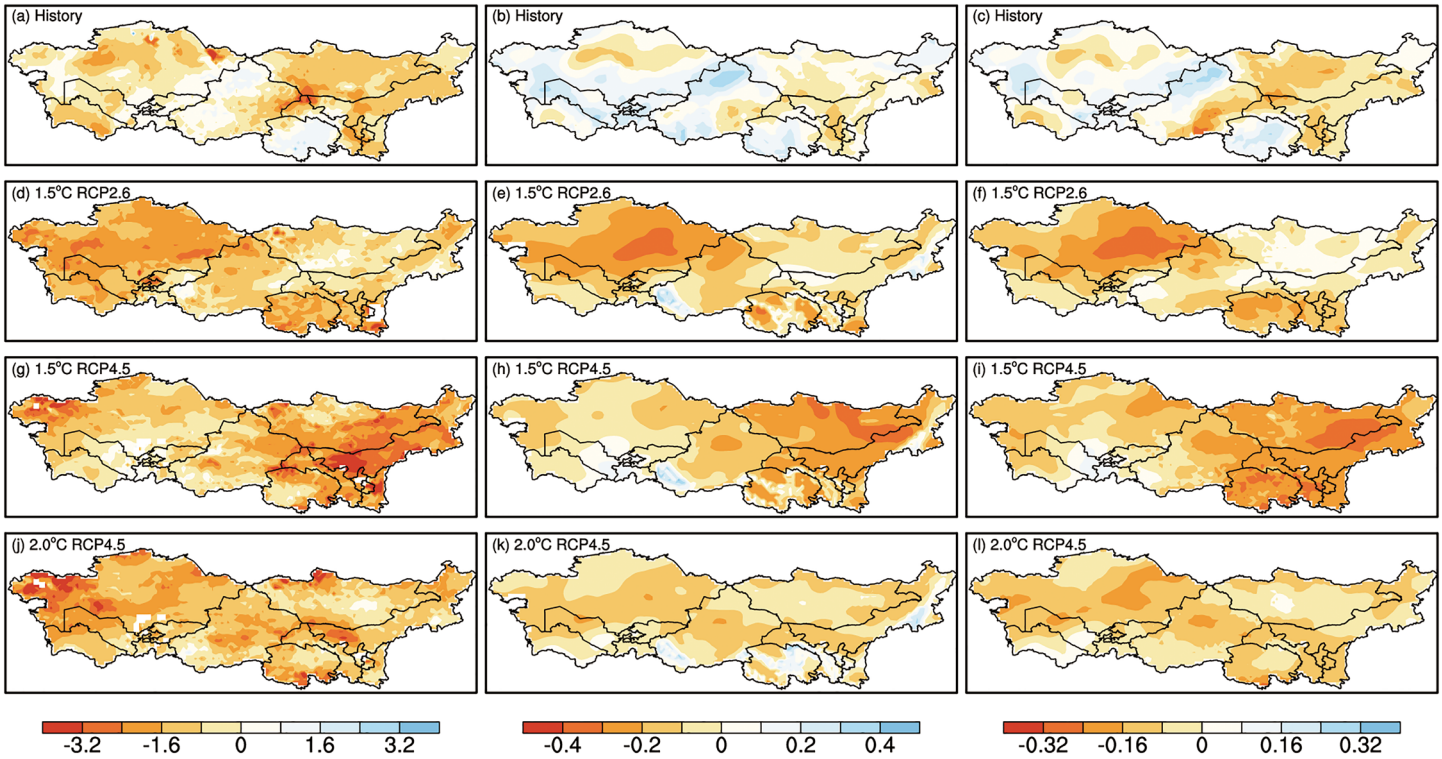


**Figure 7.** Comparison of the PDSI (a, d, g, j), SPI (b, e, h, k), and SPEI (c, f, i, l) in dryland Asia for the reference period (1986–2005) and the 1.5 °C/2.0 °C global warming periods (RCP2.6: 2020–2039/RCP4.5: 2018–2037, and RCP4.5: 2040–2059).

10.1029/2019EF001337

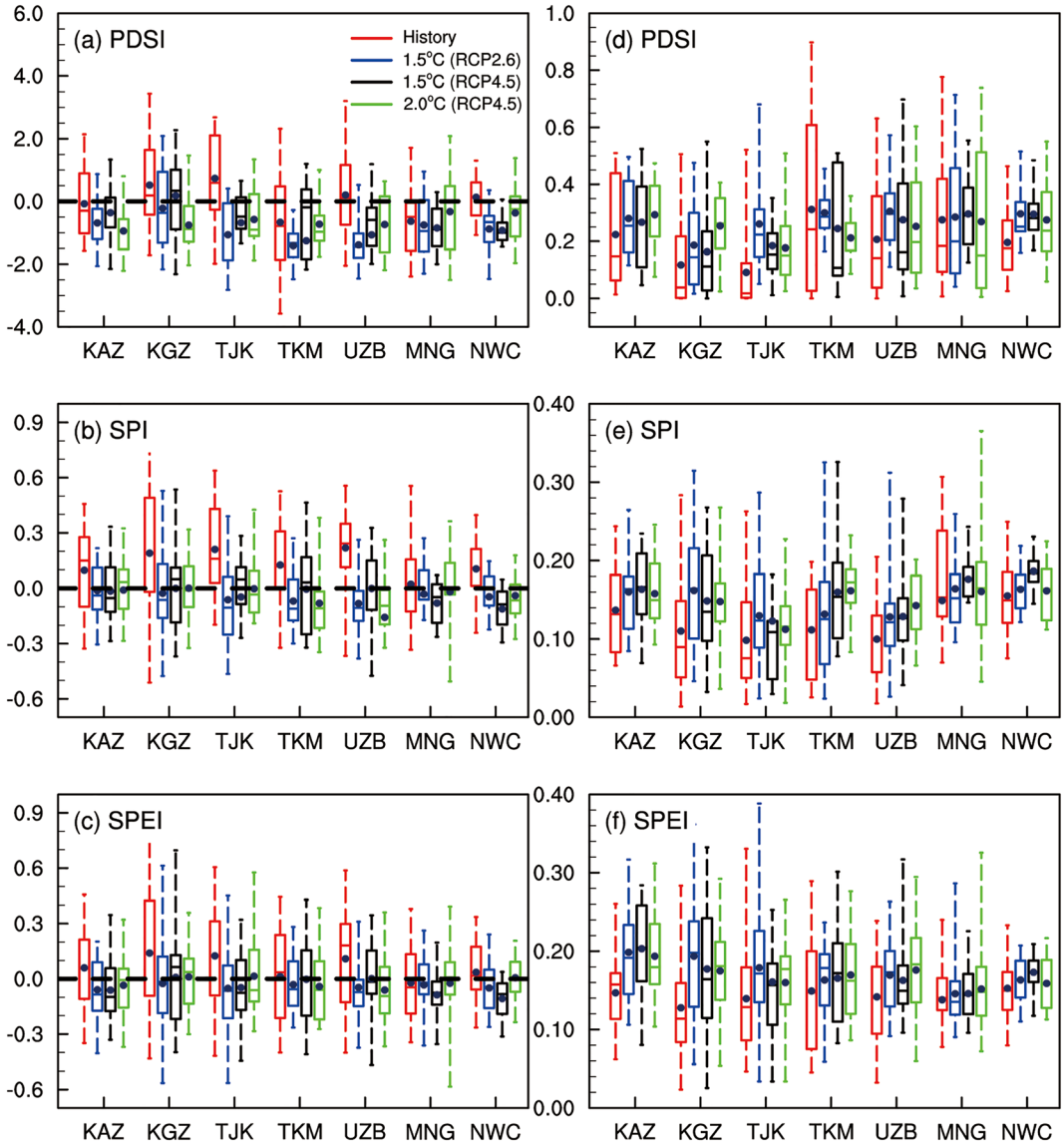


**Figure 8.** Changes in the drought intensity (a–c) and arid area (d–f), as inferred from the PDSI, SPI, and SPEI. The results averaged from seven countries/regions in dryland Asia (e.g., Kazakhstan (KAZ), Kyrgyzstan (KGZ), Tajikistan (TJK), Turkmenistan (TKM), Uzbekistan (UZB), Mongolia (MNG), and Northwest China (NWC)) are presented.

the 1.5 °C global warming scenario of RCP2.6/RCP4.5 and the 2.0 °C global warming scenario of RCP4.5 (Figure 8). The drought conditions in Kazakhstan and Northwest China are projected to be more severe in dryland Asian countries. Compared with the 1.5 °C global warming scenario, both the drought intensity and arid area will be mitigated in most of the seven countries if the temperature increases by 2.0 °C. In Mongolia, the drought level under the 2.0 °C global warming scenario from 2040–2059 will unexpectedly decrease to and even surpass the levels in the reference period (1986–2005).

## 4. Discussion and Conclusions

Using three mainstream drought indices (the PDSI, SPI, and SPEI), we estimated the drought intensity and arid area over dryland Asia under the 1.5 °C/2.0 °C global warming scenarios for future periods. Our results based on these drought indices showed that dryland Asia will experience an increasingly severe climate environment with increasing drought severity and an enlarged arid area under the 1.5 °C/2.0 °C global warming scenarios. Moreover, our findings are comparable with those in previous studies conducted in

global dryland regions and other parts of the world. Additionally, these studies revealed that a strong increase in the duration of drought under the 1.5 °C/2.0 °C/3.0 °C warming scenarios will occur in southern Africa, Australia, Brazil, Northwest China, Chile, Iran, and western and southern Asia (Huang et al., 2017; Liu et al., 2018; Naumann et al., 2018). In the Amazon, the areas exposed to mild and severe meteorological drought will nearly double and triple by 2100, respectively (Duffy et al., 2015). Similarly, most European cities will experience an increase in drought conditions under a high-impact scenario (Guerreiro et al., 2018). Thus, drought might become one of the most frequently occurring climatic extremes under future global warming conditions, which should be considered in relevant analyses.

The occurrence of drought events is complicated and generally controlled by the balance of water and energy (Granier et al., 1999). Previous studies have demonstrated that the magnitude of climate change in dryland Asia is expected to become even larger than the global average (Miao et al., 2015; Xu et al., 2019). As shown in Figure 2, dryland Asia is projected to experience increasing temperature and precipitation trends in the future. Drought conditions are closely related to changes in the water budget, which is a function of the water supplied by precipitation, surface water runoff, and local evapotranspiration. Among these factors, evapotranspiration is the major component of the water cycle and the main determinant of severe drought. The increase in evapotranspiration due to global warming will likely exacerbate droughts in dryland areas (Dai, 2012). This theory is highly applicable to the warming-induced drought variance in dryland Asia; For example, compared with the 1.5 °C global warming, the difference between precipitation and potential evapotranspiration will increase in ~60% of the region under the 2.0 °C global warming, including in eastern Kazakhstan, the eastern and western parts of Northwest China, and the eastern part of Mongolia (Figure S2). In this study, the mitigation of drought conditions under the 2.0 °C global warming, compared with those under the 1.5 °C global warming, seems perplexing and counterintuitive, but it can be explained by the above theory. For dry lands, evapotranspiration is usually several to 10 times higher than precipitation (Ran et al., 2015). The increased evaporation due to high temperatures has been the main cause of increased drought in recent years and will continue to be in the short-term future (Li et al., 2017). Under the 1.5 °C global warming scenario, the increase in precipitation is canceled out by the increase in evapotranspiration; thus, the drought conditions worsen. Nevertheless, in the 2.0 °C global warming scenario, the increases in precipitation are much greater than the increases in precipitation under the 1.5 °C warming scenario across dryland Asia. As a result, the overall drought condition becomes less severe than that in the 1.5 °C warming scenario, although the contribution of the increase in precipitation is partially offset by the increase in evaporation.

In this study, we noted that the drought conditions in Kazakhstan and Northwest China are more severe in dryland Asian countries. This result might be related to the special climate conditions in these two regions, which are characterized by low precipitation with high yearly variability. For example, the yearly precipitation variability in Kazakhstan could be dramatically influenced by large-scale oscillations under global warming (Zhang et al., 2017). These factors may lead to even more frequent and severe droughts, which in turn may threaten agricultural production in Kazakhstan—one of the major global grain producers and exporters (Feola et al., 2017). Moreover, severe and frequent droughts will increase the risk of land degradation and desertification in dryland Asia (Li et al., 2017). These findings call for short-term and long-term mitigation and adaptation measurements in dryland Asia. Thus, we support the idea that developing a dry land perspective across the continent can be an effective approach to reduce hazard risks and improve cooperation across the extensive arid land area of Asia (Sternberg, 2018).

As with any impact analysis involving climate change, uncertainty needs to be considered and constrained. The uncertainties in this study can generally be ascribed to two factors, namely, the reliability of model simulations and the drought indices involved. Large uncertainties exist in future projections of temperature and precipitation, and it might be difficult for the model to perfectly reproduce observations during the historical period. This difference reflects the gaps in our current knowledge. Thus, most studies are often conducted under specific hypothetical scenarios, but multiple models and runs are essentially needed. Selecting model results in a reasonable way is important. Multimodel ensembles are widely accepted and have been previously evaluated with satisfactory results. In this paper, however, the BMA method assigns high weights to models that have the best agreement with historical observations to obtain more reliable predictions than those obtained by simply averaging the model results.

In this study, we applied three comprehensive indices to evaluate the historical and future drought conditions in dryland Asia. Our study provided a new perspective on the consistency of the PDSI, SPI, and SPEI in reproducing the trend of historical drought conditions over dryland Asia. The BMA method was used to reproduce the drought intensity and arid area in dryland Asia based on the CRU data set and the CMIP5 models. Our findings suggest that increases in the drought intensity and area in dryland Asia will occur under future warming scenarios. Notably, the drought conditions under the 2.0 °C global warming scenario might be mitigated due to higher precipitation relative to that in the 1.5 °C global warming scenario. The findings of this study also have important implications for forecasting future climate extremes in dryland Asia; therefore, disaster emergency management and international cooperation are urgently required to respond to climate warming in the future. Understanding historical and future changes in drought conditions is critical for developing adaptation measures to cope with the challenges associated with rapid climate change and economic development. In this study, the investigation of factors that affect drought conditions mainly focuses on changes in temperature and precipitation, which cannot provide a more comprehensive attribution of drought occurrences, especially in human-oriented environments.

**Acknowledgments**
We greatly thank Prof. Dr. Tong Jiang, Prof. Dr. Zhihong Jiang from Nanjing University of Information Science and Technology, and Prof. Dr. Zhaoxin Li from Laboratoire de Météorologie Dynamique, for providing valuable comments and advices for this paper. This study was financially supported by National Key Research and Development Program of China (No. 2017YFA0603804), the European Union's Framework Programme for Research and Innovation Horizon 2020 (2014-2020) under the Marie Skłodowska-Curie Agreement (No. 795179) and the Alexander von Humboldt Foundation of Germany. We are grateful for the free open access datasets used in this study. The Climatic Research Unit (CRU) Time-Series (TS) version 4.01 was obtained from http://data.ceda.ac.uk/badc/cru/data/cru_ts/cru_ts_4.01. The CMIP5 data were obtained from https://esgf-node.llnl.gov/search/cmip5/. The authors declare no conflict of interest.

## References

Adnan, S., Ullah, K., Li, S., Gao, S., Khan, A., & Mahmood, R. (2017). Comparison of various drought indices to monitor drought status in Pakistan. *Climate Dynamics*, *51*(5–6), 1885–1899.

Bai, Y., Wu, J., Pan, Q., Huang, J., Wang, Q., Li, F., et al. (2007). Positive linear relationship between productivity and diversity: Evidence from the Eurasian Steppe. *Journal of Applied Ecology*, *44*(5), 1023–1034.

Brito, S., Cunha, A., Cunningham, C., Alvalá, R., Marengo, J., & Carvalho, M. (2018). Frequency, duration and severity of drought in the Semiarid Northeast Brazil region. *International Journal of Climatology*, *38*(2), 517–529.

Chen, J., Wan, S., Henebry, G., Qi, J., Gutman, G., Sun, G., & Kappas, M. (2013). *Dryland East Asia: Land dynamics amid social and climate change*. Beijing: Higher Education Press.

Chen, S., Gan, T. Y., Tan, X., Shao, D., & Zhu, J. (2019). Assessment of CFSR, ERA-Interim, JRA-55, MERRA-2, NCEP-2 reanalysis data for drought analysis over China. *Climate Dynamics*, *53*(1–2), 737–757.

Chen, T., Zhang, H., Chen, X., Hagan, D. F., Wang, G., Gao, Z., & Shi, T. (2017). Robust drying and wetting trends found in regions over China based on Köppen climate classifications. *Journal of Geophysical Research-: Atmospheres*, *122*, 4228–4237. https://doi.org/10.1002/2016JD026168

Dai, A. (2012). Increasing drought under global warming in observations and models. *Nature Climate Change*, *3*(1), 52–58.

Dai, A., Trenberth, K. E., & Qian, T. (2004). A global dataset of Palmer Drought Severity Index for 1870–2002: Relationship with soil moisture and effects of surface warming. *Journal of Hydrometeorology*, *5*(6), 1117–1130.

Duffy, P. B., Brando, P., Asner, G. P., & Field, C. (2015). Projections of future meteorological drought and wet periods in the Amazon. *Proceedings of the National Academy of Sciences*, *112*(43), 13172–13177.

Feola, G., Barrett, T., Khusnitdinova, M., & Krylova, V. (2017). Agricultural water use in Southeast Kazakhstan: Current challenges and adaptations to water stress. *Research Brief*, *University of Reading*.

Fraser, E. D., Dougill, A. J., Hubacek, K., Quinn, C. H., Sendzimir, J., Termansen, M. J. E., & Society (2011). Assessing vulnerability to climate change in dryland livelihood systems: Conceptual challenges and interdisciplinary solutions. *Ecology and Society*, *16*(3), 3.

Granier, A., Breda, N., Biron, P., & Villette, S. (1999). A lumped water balance model to evaluate duration and intensity of drought constraints in forest stands. *Ecological Modeling*, *116*(2–3), 269–283.

Guerreiro, S. B., Dawson, R. J., Kilsby, C., Lewis, E., & Ford, A. (2018). Future heat-waves, droughts and floods in 571 European cities. *Environmental Research Letters*, *13*(3), 034009.

He, B., Wang, S., Guo, L., & Wu, X. (2019). Aridity change and its correlation with greening over drylands. *Agricultural and Forest Meteorology*, *278*, 107663.

Hoeting, J. A., Madigan, D., Raftery, A. E., & Volinsky, C. T. (1999). Bayesian model averaging: A tutorial. *Statistical Science*, 382–401.

Hu, Z., Zhang, C., Hu, Q., & Tian, H. (2014). Temperature changes in Central Asia from 1979 to 2011 based on multiple datasets. *Journal of Climate*, *27*(3), 1143–1167.

Huang, J., Yu, H., Dai, A., Wei, Y., & Kang, L. (2017). Drylands face potential threat under 2 °C global warming target. *Nature Climate Change*, *7*(6), 417.

Huang, J., Yu, H., Guan, X., Wang, G., & Guo, R. (2016). Accelerated dryland expansion under climate change. *Nature Climate Change*, *6*(2), 166.

Huang, J., Zhai, J., Jiang, T., Wang, Y., Li, X., Wang, R., et al. (2018). Analysis of future drought characteristics in China using the regional climate model CCLM. *Climate Dynamics*, *50*(1–2), 507–525.

IPCC. (2013). *Climate change 2013—The physical science basis: Summary for policymakers, intergovernmental panel on climate change*. Geneva, Switzerland.

Jones, P., & Harris, I. (2013). Climatic research unit (CRU) timeseries (TS) version 3.21 of high resolution gridded data of month-by-month variation in climate (Jan. 1901–Dec. 2012). *NCAS British Atmospheric Data Centre*.

King, A. D., Karoly, D. J., & Henley, B. J. (2017). Australian climate extremes at 1.5 °C and 2 °C of global warming. *Nature Climate Change*, *7*(6), –412.

Lehner, F., Coats, S., Stocker, T., Pendergrass, A., Sanderson, B., Raible, C., & Smerdon, J. (2017). Projected drought risk in 1.5 °C and 2 °C warmer climates. *Geophysical Research Letters*, *44*, 7419–7428. https://doi.org/10.1002/2017GL074117

Li, Z., Chen, Y., Fang, G., & Li, Y. (2017). Multivariate assessment and attribution of droughts in Central Asia. *Scientific Reports*, *7*(1), 1316.

Liu, R., Jacobi, C., Hoffmann, P., Stober, G., & Merzlyakov, E. (2010). A piecewise linear model for detecting climatic trends and their structural changes with application to mesosphere/lower thermosphere winds over Collm, Germany. *Journal of Geophysical Research*, *115*, D22105. https://doi.org/10.1029/2010JD014080

Liu, W., Sun, F., Lim, W. H., Zhang, J., Wang, H., Shiogama, H., & Zhang, Y. (2018). Global drought and severe drought-affected populations in 1.5 and 2 °C warmer worlds. *Earth System Dynamics*, *9*(1), 267–283.

Liu, Z., Wang, Y., Shao, M., Jia, X., & Li, X. (2016). Spatiotemporal analysis of multiscalar drought characteristics across the Loess Plateau of China. *Journal of Hydrology*, *534*, 281–299.

Meinshausen, M., Meinshausen, N., Hare, W., Raper, S. C., Frieler, K., Knutti, R., et al. (2009). Greenhouse-gas emission targets for limiting global warming to 2 °C. *Nature*, *458*(7242), 1158.

Miao, L., Fraser, R., Sun, Z., Sneath, D., He, B., & Cui, X. (2015). Climate impact on vegetation and animal husbandry on the Mongolian Plateau: A comparative analysis. *Natural Hazards*, *80*(2), 727–739.

Miao, L., Ye, P., He, B., Chen, L., & Cui, X. (2015). Future climate impact on the desertification in the dry land Asia using AVHRR GIMMS NDVI3 g data. *Remote Sensing*, *7*(4), 3863–3877.

Nangombe, S., Zhou, T., Zhang, W., Wu, B., Hu, S., Zou, L., & Li, D. (2018). Record-breaking climate extremes in Africa under stabilized 1.5 °C and 2 °C global warming scenarios. *Nature Climate Change*, *8*(5), –375.

Naumann, G., Alfieri, L., Wyser, K., Mentaschi, L., Betts, R., Carrao, H., et al. (2018). Global changes in drought conditions under different levels of warming. *Geophysical Research Letters*, *45*, 3285–3296. https://doi.org/10.1002/2017GL076521

Noah, S. D., & Filippo, G. (2012). Climate change hotspots in the CMIP5 global climate model ensemble. *Climatic Change*, *114*(3–4), 813–822.

Ran, M., Zhang, C., & Feng, Z. (2015). Climatic and hydrological variations during the past 8000 years in northern Xinjiang of China and the associated mechanisms. *Quaternary International*, *358*, 21–34.

Sneath, D. (1999). *The end of Nomadism?: Society, state, and the environment in Inner Asia*. Durham: Duke University Press.

Sternberg, T. (2018). Moderating climate hazard risk through cooperation in Asian drylands. *Land*, *7*(1), 22.

Su, B., Huang, J., Fischer, T., Wang, Y., Kundzewicz, Z. W., Zhai, J., et al. (2018). Drought losses in China might double between the 1.5 °C and 2.0 °C warming. *Proceedings of the National Academy of Sciences*, *115*(42), 10600–10605.

Svoboda, M., Hayes, M., & Wood, D. (2012). *Standardized precipitation index user guide*. Switzerland: World Meteorological Organization Geneva.

Tao, S., Fang, J., Zhao, X., Zhao, S., Shen, H., Hu, H., et al. (2015). Rapid loss of lakes on the Mongolian Plateau. *Proceedings of the National Academy of Sciences*, *112*(7), 2281–2286.

Thornthwaite, C. W. (1948). An approach toward a rational classification of climate. *Geographical Review*, *38*(1), 55–94.

Tian, L., Yuan, S., & Quiring, S. M. (2018). Evaluation of six indices for monitoring agricultural drought in the south-central United States. *Agricultural and Forest Meteorology*, *249*, 107–119.

Trenberth, K., Dai, A., van der Schrier, G., Jones, P., Barichivich, J., Briffa, K., & Sheffield, J. (2013). Global warming and changes in drought. *Nature Climate Change*, *4*(1), 17–22.

Wang, J., Brown, D., & Agrawal, A. (2013). Climate adaptation, local institutions, and rural livelihoods: A comparative study of herder communities in Mongolia and Inner Mongolia, China. *Global Environmental Change*, *23*(6), 1673–1683.

Wayne, C. (1965). *Meteorological drought*, (Vol. 45, p. 58). Washington DC: Research Paper, Office of Climatology, Weather Bureau.

Wei, Y., Yu, H., Huang, J., Zhou, T., Zhang, M., & Ren, Y. (2019). Drylands climate response to transient and stabilized 2 ° C and 1.5 ° C global warming targets. *Climate Dynamics*, *53*(3–4), 2375–2389.

Xu, H., Zhou, K., Lan, J., Zhang, G., & Zhou, X. (2019). Arid central Asia saw mid-Holocene drought. *Geology*, *47*(3), 255–258.

Zhang, R., Shang, H., Yu, S., He, Q., Yuan, Y., Bolatov, K., & Mambetov, B. (2017). Tree-ring-based precipitation reconstruction in southern Kazakhstan, reveals drought variability since AD 1770. *International Journal of Climatology*, *37*(2), 741–750.